European Journal of Pharmaceutics and Biopharmaceutics 71 (2009) 271–281

Contents lists available at ScienceDirect

European Journal of Pharmaceutics and Biopharmaceutics

journal homepage: www.elsevier.com/locate/ejpb

Research paper

Intraorally fast-dissolving particles of a poorly soluble drug: Preparation and in vitro characterization

Riikka Laitinen [a,*], Eero Suihko [a,1], Kaisa Toukola [a], Mikko Björkqvist [b], Joakim Riikonen [b], Vesa Pekka Lehto [b], Kristiina Järvinen [a], Jarkko Ketolainen [a]

[a] Department of Pharmaceutics, University of Kuopio, Kuopio, Finland
[b] Laboratory of Industrial Physics, Department of Physics, University of Turku, Turku, Finland

ARTICLE INFO

Article history:
Received 21 May 2008
Accepted in revised form 2 September 2008
Available online 12 September 2008

Keywords:
Solid dispersion
Solid solution
Dissolution enhancement
PVP
PEG
Amorphous

ABSTRACT

In this study, the dissolution rate of a poorly soluble drug, perphenazine (PPZ) was improved by a solid dispersion technique to permit its usage in intraoral formulations. Dissolution of PPZ (4 mg) in a small liquid volume (3 ml, pH 6.8) within one minute was set as the objective. PVP K30 and PEG 8000 were selected for carriers according to the solubility parameter approach and their 5/1, 1/5 and 1/20 mixtures with PPZ (PPZ/polymer w/w) were prepared by freeze-drying from 0.1 N HCl solutions. The dissolution rate of PPZ was improved with all drug/polymer mixture ratios compared to crystalline or micronized PPZ. A major dissolution rate improvement was seen with 1/5 PPZ/PEG formulation, i.e. PPZ was dissolved completely within one minute. SAXS, DSC and XRPD measurements indicated that solid solutions of amorphous PPZ in amorphous PVP or in partly amorphous PEG were formed. DSC and FTIR studies suggested that PPZ dihydrochloride salt was formed and hydrogen bonding was occurred between PPZ and the polymers. It was concluded that molecular mixing together with salt formation promoted the dissolution of PPZ, especially in the case of the 1/5 PPZ/PEG dispersion, making it a promising candidate for use in intraoral formulations.

1. Introduction

Drug delivery via the oral mucosa is a promising route, when one wishes to achieve a rapid onset of action or improved bioavailability for drugs with high first-pass metabolism [1]. Thus, there is a growing interest in developing alternative dosage forms, i.e. orally fast disintegrating tablets, which allow a rapidly dissolving drug to absorb directly into the systemic circulation through the oral mucosa. These kinds of dosage forms are also convenient for children, elderly patients with swallowing difficulties, and in the absence of potable liquids [2]. However, in addition to formulation considerations, the properties of the active compound have to be appropriate in order to achieve drug delivery into systemic circulation after intraoral administration. The drug has to be soluble, fast dissolving and stable, and this might represent an obstacle for lipophilic drugs [3]. Due to the small volume of saliva in the oral cavity, the therapeutic dose of an intraoral drug must be relatively small and in most cases dissolution enhancers must be applied [4]. To overcome these problems, a solid dispersion approach can be utilized.

Solid dispersions are generally prepared by incorporating the drug into a water soluble carrier using techniques like solvent evaporation or melt extrusion. The improvement of drug dissolution from solid dispersions is attributed to drug particle size reduction and possible amorphization within the dispersion, improved wetting of the drug, as well as a possible solubilization effect of the carrier and specific molecular interactions between the drug and polymer [5,6]. Depending on the solid state solubility of the drug in a polymer, either a suspension or a molecular dispersion of the drug in the polymer matrix can result. In the former, clusters of either amorphous or crystalline drug are present, thus a phase-separated system will result. In the latter case, the drug is homogenously dispersed in a carrier matrix and its size is at an absolute minimum, which is beneficial for the dissolution rate [5]. Molecular-level mixing can be achieved either by dissolving each component in a mutually common solvent followed by solvent removal or by directly mixing the two liquids if the drug and the carrier are miscible with each other [7,8]. However, in spite of intensive research in the field of solid dispersions, dispersion of the drug and its particle size within a polymer matrix are rarely studied. Microscopic methods have been used for this purpose, however they are not able to detect molecular dispersions [9–11]. Instead, alternative techniques such as micro-Raman [12] and potential new methods, such as Small-angle X-ray scattering (SAXS) [13] could be used.

* Corresponding author. Department of Pharmaceutics, University of Kuopio, P.O. Box 1627, FI-70211 Kuopio, Finland. Tel.: +358 40 355 3881; fax: +358 17 162 252.
E-mail address: riikka.laitinen@uku.fi (R. Laitinen).
[1] Present address: Orion Corporation, P.O. Box 1780, FI-70701 Kuopio, Finland.

0939-6411/$ - see front matter © 2008 Elsevier B.V. All rights reserved.
doi:10.1016/j.ejpb.2008.09.001

PVP and PEG are the most commonly used carriers in solid dispersions [9–12,14,15]. PVP has been reported to form amorphous solid dispersions and solutions with many drugs [7,9,14,16]. In contrast, only a few compounds have been observed to form amorphous solid dispersions with PEG [15]. However, PEG–drug interactions leading to destruction of the crystal lattice of the drug and a partial disruption of the carrier lattice, i.e. to formation of solid solutions, have been also reported [17], but only at relatively low drug concentrations [15,18].

The best reported dissolution rates so far from PVP or PEG matrices have been at the level of 100% of drug dissolved in 15–20 min in sink conditions [10,19] which is too slow to allow adequate absorption for drugs in the oral cavity [3]. Thus, the aim of this study was to achieve considerable enhancement of the dissolution rate of perphenazine (PPZ), i.e. the target was to achieve 100% of PPZ dose (4 mg) dissolved within one minute. PPZ (M_W = 404, pK_a = 7.8 and log$P$ = 3.1) is a practically water insoluble drug, used as an antipsychotic with a daily dose of 12–24 mg [20]. To accomplish the abovementioned goal, molecular-level mixing was utilized. This entails the formation of a solid solution of PPZ with polymers (i.e. PVP K30 and PEG 8000), selected based on the similarity of their solubility parameter values with that of PPZ. Freeze-drying was used for the creation of the dispersions with drug/polymer ratios 5/1, 1/5 and 1/20 (w/w). The dissolution rate of the prepared dispersions was determined in a small liquid volume in order to evaluate their dissolution in oral cavity. As far as we are aware, SAXS was used for the first time for studying the distribution of the drug in the polymer matrices and the formation of PPZ/polymer solid solutions. The dispersions were further characterized by SEM (Scanning Electron Microscopy), DSC (Differential Scanning Calorimetry), XRPD (X-ray Powder Diffraction) and FTIR (Fourier Transform Infrared Spectroscopy).

2. Materials and methods

2.1. Materials

Perphenazine [PPZ, USP, d(0.5) = 30 μm)], PVP K30 (purum) and PEG 8000 (SigmaUltra) were purchased from Sigma Aldrich (Sigma–Aldrich Chemie, Steinheim, Germany). Since PPZ is photosensitive, all PPZ containing powders and solutions were protected from light during processing. For the dissolution studies, micronized PPZ (<15 μm fraction) was prepared by grinding and sieving through a 15 μm sieve mesh. All other materials used were of analytical grade.

The polymer selection was based on a comparison of the solubility parameter of PPZ [estimated according to the group contribution method [21] using the Matprop©-program (Material Property Estimator and Database, SF Technologies, Amherst, MA)] to the solubility parameters of different polymers and polymer grades, found in the literature [8,22–24]. The solubility parameter (δ) is a way to quantify the cohesive energy of a material, which in turn determines many of the critical physico-chemical properties (e.g. solubility, melting point) of drugs and excipients. It can be used in order to predict the miscibility of drugs and excipients [8,23,24]. Several group contribution methods have been developed for calculating solubility parameters [25]. This approach requires knowledge of the chemical structure of the material but this information is normally available for pharmaceutical materials. In the Hansen solubility parameter [22], which can be estimated based on the method of Hoftyzer/Van Krevelen [25], the dispersive forces, interactions between polar and hydrogen bonding groups are taken into account.

2.2. Preparation of the solid dispersions

Solid dispersions with different drug/polymer-weight ratios (5/1, 1/5 and 1/20) were prepared by freeze-drying. Thus, the dispersions contained 80, 20 and 5% of PPZ, respectively. Also pure PPZ was processed similarly. PPZ (pK_a 7.8) was found to dissolve sufficiently in 0.1 N HCl solution (39.5 ± 0.2 mg/ml), thus 0.1 N HCl was used as a solvent in this procedure. For the freeze-drying, 0.1 N HCl solutions with an overall solid concentration (drug + polymer) of 5% (w/w) in the case of 1/5 and 1/20 dispersions were prepared, 3% solutions in the case of 5/1 dispersions and 2% solutions in the case of pure PPZ. The solutions were poured into 20 ml portions in beakers and transferred into a freezer (−80 °C, Vip Series 86, Sanyo Electric Biomedical Co. Ltd., Wood Dale, IL). After freezing, the samples were freeze-dried (Modulyod-230, Thermo Savant, Savant NY) for 2–4 days. The prepared particles were stored in desiccator over silica gel at a temperature below 10 °C.

2.3. Solubility studies

2.3.1. Perphenazine assay

The concentrations of PPZ were determined by HPLC with UV-detection at the wavelength of 254 nm. The Gilson HPLC system consisted of 234 Autoinjector (Gilson, Roissy en France, France), 321 Pump, UV/vis-151 Detector, System interface module and Unipoint™ LC system version 3.01 software (all from Gilson, Middleton, WI). A reverse-phase column (Inertsil ODS-3, 4.0 ∗ 150 mm, GL Sciences Inc., Tokyo, Japan) was used. The sample injection volume was 20 μl, the mobile phase was acetonitrile-water (70/30) with 0.03% (v/v) triethylamine (TEA), and its flow rate was 1 ml/min. The retention time of PPZ was 3.75 ± 0.25 min. The PPZ standards were prepared in 70/30 acetonitrile/buffer solution (buffer being pH 1.2 or 6.8, depending on which buffer was used in the solubility study at the time). The standard curve was linear (r^2 > 0.997) over the range of concentrations of interest (0.1–100 μg/ml). The repeatability of the HPLC method was tested by analyzing the 25 μg/ml standard solution five times in a row before every analysis. The RSD of the peak area was always <3%.

2.3.2. Determination of solubility and dissolution rate

The PPZ equilibrium solubility at pH 6.8 was determined by adding excess amounts of the drug to 1 ml of buffer solution (pH unchanged during the experiment) at room temperature. The suspensions were equilibrated in a shaker (at speed 300 rpm) for three days and then filtered through a 0.45 μm membrane filter. For the phase-solubility studies, solutions containing 10, 7.5, 5, 2.5 and 1% (w/v) of PVP or PEG in pH 6.8 phosphate buffer (pH was unchanged during the experiment) were prepared. Otherwise the phase-solubility study was carried out similarly as the solubility studies, with the exception that the solution volume was 10 ml. A 150 μl sample of the filtered test solution was taken, mixed with 350 μl of ACN and analyzed with HPLC.

The dissolution rates of the materials were determined in a small volume (3 ml of pH 6.8 phosphate buffer), in order to simulate the small liquid volumes present in the mouth. The powder was weighed in the bottom of the test tubes in such a way that there was always 4 mg of PPZ. Three parallel samples were prepared for each time point. The test tubes were placed on a shaker at the speed of 300 rpm (KS125basic, IKA Labortechnik, IKA-Werke Gmbh and Co., Straufen, Germany) and 3 ml of the pH 6.8 buffer was added to the test tube. The samples were taken at 15, 30 and 45 s, 1, 2 and 4 min time points by pouring the solution into a syringe equipped with a 0.45 μm membrane filter on the head, filtering it immediately and diluting it with phosphate buffer prior to analysis with HPLC. The dissolution rates of PPZ (d(0.5) = 30 μm) and PPZ micronized (<15 μm) were also determined under sink

conditions (i.e. the PPZ sample amount was such that the maximum amount of the dissolved PPZ was 5% of its equilibrium solubility) using the USP XXVIII rotating paddle method, with a rotation speed of 50 rpm (Sotax AT 6 dissolution tester, Sotax AG, Basel, Switzerland). The dissolution medium (900 ml of pH 6.8 phosphate buffer) was maintained at 37.0 ± 0.5 °C.

2.4. Physical characterization of the dispersions

2.4.1. Small-angle X-ray scattering

In SAXS, the X-ray radiation generated by PW 1830 X-ray generator (Philips, Amelo, The Netherlands, operated at 40 kV and 50 mA) was limited to a narrow line. This permitted determination of scattering of the radiation which penetrated through the sample starting from small angles. The intensity of the scattered radiation was measured by a proportional counter by changing the angle stepwise (Kratky-camera, Anton Paar, Graz, Austria). The measuring times were approximately 20 h per sample (5 min/step). The measurements were carried out by measuring the scattering of the transmitted radiation at small angles (starting from as small angles as possible). Background and a few measuring points from the beginning of the measured data were removed (since their intensity was affected by the stopper of the primary beam). When analyzing the data, the shape of the areas of different electron densities (i.e. particles) were assumed to be spherical and their size distribution was estimated to be from 0 to 100 nm. The pair density distribution (POR) functions, determined from the original data, provide information on the size of the electron density areas in the sample. The maximum values of the functions are not comparable with each other due to the varying sample sizes. Instead, the place of the maximum (nm) is in this case more informative.

2.4.2. Scanning electron microscopy

The samples were pretreated by placing them onto sample stubs and coated with gold (Polar Sputter Coater II-E5100, Polaron Equipment Ltd., Watford, UK). The SEM micrographs were taken with a XL 30 ESEM TMP microscope (FEI Co., Czech Republic). The accelerating voltage was 20 kV.

2.4.3. Differential scanning calorimetry

Thermal behavior of the materials was studied with a Mettler Toledo DSC823[e] equipped with an intercooler (Mettler Toledo, Schwerzenbach, Switzerland) and an autosampler (Mettler Toledo, TS080IRO, Sample Robot, Schwerzenbach, Switzerland). The cooling/heating programs when measuring the melting points (T_m) and glass transition temperatures (T_g) for the different samples are shown in Table 1. Since PVP is very hygroscopic, the overlying water evaporation endotherm had to be separated from the other thermal events, such as glass transition, by sine-wave temperature modulation in the case of 1/5- and 1/20 PPZ/PVP-formulations (Table 1). The samples were weighed (weight range 2–11 mg) with an analytical balance (Mettler Toledo AT261, Mettler Toledo Ag, Schwerzenbach, Switzerland) and analyzed in sealed 40 μl aluminium sample pans (Mettler Toledo, Schwerzenbach, Switzerland) with a pierced lid. Measurements for each material were performed in triplicate. H_2O, In, Pb and Zn were used for temperature scale and enthalpy response calibration, however, for the temperature modulated runs, no further calibration was done, thus the ΔC_p-values could not be compared between the different materials. Results were analysed with STAR[e] software (Mettler Toledo Schwerzenbach, Switzerland). Melting points were determined as onset-values and the glass transition temperatures as midpoint-values. In the case of temperature modulated measurements, the T_g-values were determined from the reversing heat flow signal as midpoint-values.

2.4.4. X-ray powder diffraction

X-ray powder diffraction analysis (XRPD) was performed using a Philips PW 1830 diffractometer (Philips, Amelo, The Netherlands) with Bragg-Brentano geometry (θ–2θ). The radiation used was nickel filtered CuK_α, which was generated using an acceleration voltage of 40 kV and a cathode current of 50 mA. The samples were scanned over a 2θ range of 3°–30°, step size being 0.04° and counting time 3 s per step.

2.4.5. Fourier transform infrared spectroscopy

A Nicolet Nexus 870 FTIR spectrometer (Thermo Electron Corp, Madison, WI) equipped with an Attenuated Total Reflectance (ATR) accessory (Smart Endurance, Single-reflection ATR diamond composite crystal) was used for obtaining the IR-spectra. For each spectrum, 32 scans were performed with a resolution of 4 cm^{-1}. For the physical mixtures and the dispersions, three samples were measured and their average spectra were calculated.

3. Results

3.1. Improvement of PPZ dissolution rate

In conditions simulating the buccal cavity [i.e. low liquid volume (3 ml), with pH 6.8 (unchanged at the end of the experiment)], the solubility of PPZ was found to be low, i.e. 149 ± 3 μg/ml. In addition, the dissolution rate was poor, i.e. within 4 min only 2% of PPZ had dissolved (Fig. 1a). Reducing the particle size of PPZ

Table 1
DSC cooling/heating programs for the starting materials (perphenazine (PPZ), PVP K30 and PEG 8000), freeze-dried perphenazine, solid dispersions (drug/polymer-ratio 5/1, 1/5 and 1/20) and the corresponding physical mixtures

Sample	Phase 1 (heating)	Phase 2 (cooling)	Phase 3 (heating)	Temperature modulation
PPZ	From 25 °C to 115 °C, 10 °C/min	From 115 °C immediately to −40 °C, 15 min at −40 °C	From −40 °C to 120 °C, 10 °C/min	–
PVP K30	From 25 °C to 140 °C, 10 °C/min, 10 min at 140 °C	From 140 °C immediately to 25 °C, 10 min at 25 °C	From 25 °C to 190 °C, 10 °C/min	–
PEG 8000	From 25 °C to 100 °C, 10 °C/min, 3 min at 100 °C	from 100 °C to -75 °C, 10 °C/min, 15 min at −75 °C	From −75 °C to 100 °C, 10 °C/min	–
Freeze-dried PPZ, 5/1 PPZ/PVP physical mixture and solid dispersion	From 0 °C to 125 °C, 10 °C/min	–	–	–
1/5 and 1/20 PPZ/PVP physical mixture and solid dispersion	From 0°C to 200°C, 1°C/min	–	–	Amplitude ± 1°C, frequence 1 min
5/1 PPZ/PEG physical mixture and solid dispersion	–	At −40 °C 10 min	From −40 °C to 55 °C or to 125 °C, 10 °C/min	–
1/5 and 1/20 PPZ/PEG physical mixture and solid dispersion	–	At −75 °C 30 min	From −75 °C to −10 °C or to 125 °C, 10 °C/min	–

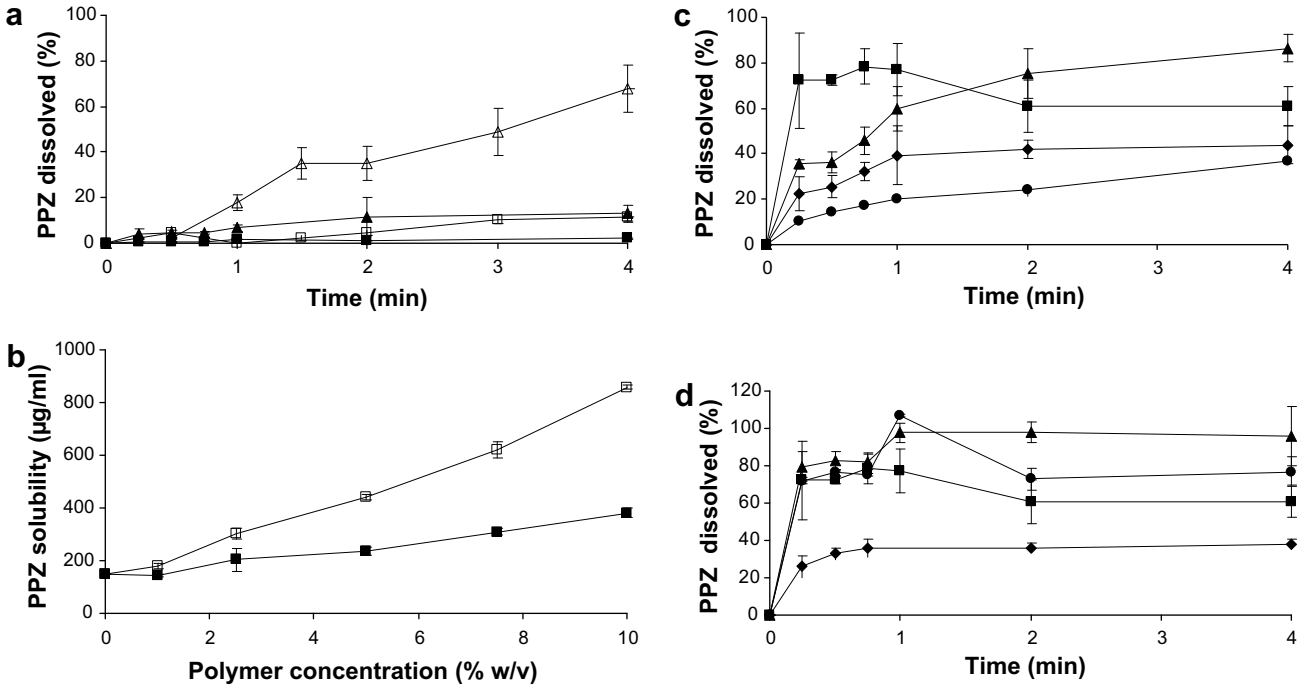

Fig. 1. Dissolution curves of (a) PPZ ($d(0.5)$ = 30 µm) in supersaturated (■) and sink conditions (□), and micronized (<15 µm) PPZ in supersaturated (▲) and sink conditions (△); (b) phase-solubility diagrams of PPZ in solutions PVP (□) and PEG (■) in pH 6.8 buffer at room temperature; (c) dissolution curves of freeze-dried PPZ (■) and PPZ/PVP solid dispersions [5/1 (♦), 1/5 (▲) and 1/20 (•)] in supersaturated conditions and (d) dissolution curves of freeze-dried PPZ (■) and PPZ/PEG solid dispersions [5/1 (♦), 1/5 (▲) and 1/20 (•)] in supersaturated conditions. Error bars indicate the standard deviation (n = 3).

did not markedly change the situation, viz. only 13% of PPZ < 15 µm had dissolved within 4 min. Furthermore, even when sink conditions prevailed a mere 12% of PPZ and 68% of PPZ < 15 µm dissolved within 4 min (Fig. 1a) and 43% of PPZ and 88% of PPZ < 15 µm after 20 min (results not shown).

In a solid solution of a drug in a polymer, the drug size is at its absolute minimum, allowing the drug to be present as individual molecules in solution as the polymer dissolves which leads to improved dissolution rate of the drug [5,6]. It is known that materials with similar solubility parameters will have similar intermolecular interactions, which will favor miscibility [26]. It has been demonstrated that compounds with a solubility parameter difference ($\Delta\delta$) smaller than 7.0 $MPa^{1/2}$ are likely to be miscible with each other, and when $\Delta\delta$ is smaller than 2.0 $MPa^{1/2}$ the components might form a solid solution [8,22]. Thus, in this study, the solubility parameter approach [8,22–24,27] was used for predicting the miscibility of PPZ with different polymers and the possible ability of the components to form a solid solution with each other. The δ value for PPZ was estimated to be 22.4 $MPa^{1/2}$. Evaluation of a wide selection of polymers and their different grades [8,22–24] revealed that from hydrophilic polymers PVPs and PEGs had the solubility parameter values nearest to that of PPZ. The polymer grades of PVP K 30 and PEG 8000 with δ-values of 22.4 ($\Delta\delta$ = 0) and 21.6 $MPa^{1/2}$ ($\Delta\delta$ = 0.8) [8], respectively, were found to provide the most favorable conditions for molecular-level mixing with PPZ.

In phase-solubility studies, increasing concentrations of PVP and PEG were found to increase linearly the PPZ solubility in pH 6.8 buffer, however, PVP considerably more than PEG (Fig. 1b) as observed previously for the other model drugs [28–30].

The dissolution rate of freeze-dried PPZ, and PPZ from prepared PPZ/PVP and PPZ/PEG dispersions was determined in a small volume (3 ml). Thus, the dissolution of PPZ would result in supersaturated conditions (i.e. maximum 9-times the equilibrium solubility of crystalline PPZ). This was clearly seen in the case of freeze-dried PPZ which dissolved very rapidly at the beginning (nearly 80% of PPZ dissolved already after 15 s), PPZ concentration exceeding PPZ equilibrium solubility over 7-fold (Fig. 1c). However, the supersaturated PPZ started to precipitate after one minute and the amount of dissolved PPZ declined down to 60% dissolved.

In the case of PPZ/polymer dispersions, dissolution studies in supersaturated conditions provide information about the maximum PPZ concentrations and the cumulative supersaturation, which depend on the dissolution of the powder and the ability of polymer to inhibit precipitation of PPZ. In the case of PPZ/PVP dispersions (Fig. 1c), no precipitation of supersaturated PPZ was observed due to the effect of PVP to increase PPZ solubility (Fig. 1b). After 15 s, 20, 35 and 10% of PPZ had dissolved from 5/1, 1/5 and 1/20 PPZ/PVP, respectively, increasing up to 40%, 90% and 30% after 4 min.

In the case of PPZ/PEG formulations, no precipitation of the supersaturated PPZ was observed with 5/1 and 1/5 formulations. However, only 40% of PPZ dissolved from the 5/1 PPZ/PEG after 4 min. Instead, in the case of 1/5 and 1/20 PPZ/PEG, all of the PPZ dissolved within one minute (Fig. 1d), but in the case of 1/20-formulation, the amount of PPZ dissolved declined to 80% after the 2 min time point, for which no obvious explanation was found.

3.2. Physical characterization of the solid dispersions

3.2.1. Determination of PPZ distribution in the polymer matrices by SAXS

Small-angle X-ray scattering (SAXS) measurements are performed by focusing the X-ray beam onto a sample and observing the coherent scattering pattern that arises from the electron density inhomogeneities within the sample. This variation in electron density can be divided into two categories: the deviation resulting from the atomic structure of each of the phases and that attributable to the heterogeneity of the material. The amount and angular distribution of the scattered intensity provides information, such as the size of very small particles or their surface area per unit vol-

ume, regardless of whether the sample or particles are crystalline or amorphous. SAXS patterns are caused by the existence of inhomogeneity regions of sizes of several nanometers to several tens of nanometers, whereas XRD is able to determine the atomic structures. SAXS permits the measurement of the size of inhomogeneity regions in the range from 1 to 100 nm and it has many uses in the diverse fields from the evaluation of biological structure to examination of dispersoids in structural engineering materials, for example in the characterization of the nanocrystals [13,31,32].

In this study, SAXS measurements for the 1/5 and 1/20 PPZ/PVP and PPZ/PEG solid dispersions were carried out in order to study the distribution of the component particles in the dispersions and the possible formation of PPZ solid solution. Similarly processed PVP and PEG were used as reference samples. Areas with dimensions of 50–100 nm can be considered as drug particles that have not achieved molecular-level dispersion in the polymer [12]. However, these kinds of PPZ areas did not appear, since the curve shape and the location of the maximum in the pair density distribution functions did not seem to be affected in spite of addition of PPZ, or the amount of the added PPZ. In the curves of PVP, PEG and their 1/5 and 1/20 dispersions with PPZ one large maximum around 25 nm and another much smaller around 90 nm can be seen (Fig. 2a and b, Table 2). Furthermore, no differences between 1/5 and 1/20 dispersions were observed.

3.2.2. Evaluation of changes in the physical state of the materials by SEM, XRPD and DSC

SEM micrographs reveal clear changes in the morphology of the powder particles due to the evident formation of solid dispersions. In physical mixtures, separate PPZ (flaky) and polymer particles (spherical) are clearly seen (Fig. 3a and b). Instead, the solid dispersions exhibited the appearance of typical, flaky freeze-dried material (Fig. 3c and d). Based on SEM, no considerable differences in the particle sizes of the 1/5 (Fig 3c and d) and 1/20 PPZ/polymer dispersions (not shown) were observed. The particle size of 5/1 PPZ/polymer dispersions seemed to be slightly smaller (not shown). However, the visually observed increase in the surface area of the material and closer contact between the hydrophilic polymers and PPZ (Fig. 3c and d) compared to the corresponding characteristics in the physical mixtures (Fig. 3a and b) may well be factors resulting in faster dissolution of the drug [33].

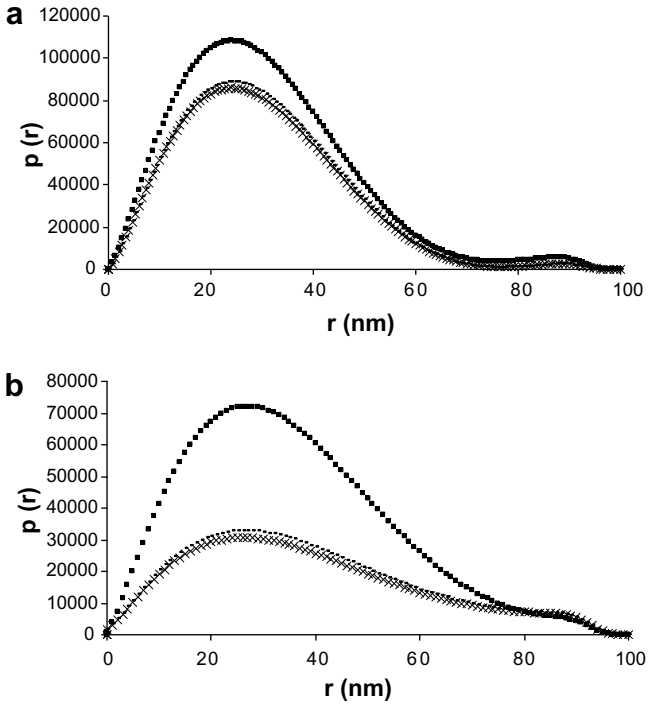

Fig. 2. Pair density distribution functions of (a) freeze-dried PVP (■) and 1/5 (x) and 1/20 PPZ/PVP (–) solid dispersions; (b) freeze-dried PEG (■) and 1/5 (x) and 1/20 PPZ/PEG (–) solid dispersions, determined from SAXS measurements.

Table 2
Maxima of the size distribution of the inhomogeneity regions in 1/5 and 1/20 PPZ/polymer dispersions and similarly processed polymers, determined by SAXS

Sample	1. Peak maximum (nm)	2. Peak maximum (nm)
Freeze-dried PVP	24	88
1/5 PPZ/PVP solid dispersion	24	70
1/20 PPZ/PVP solid dispersion	24	89
Freeze-dried PEG	27	80
1/5 PPZ/PEG solid dispersion	26	80
1/20 PPZ/PEG solid dispersion	26	80

Changes in the physical state of the materials due to the formation of solid dispersion were further studied by XRPD. The diffraction pattern of pure PPZ with several characteristic peaks confirmed that the drug was crystalline (Fig. 4a). In addition, PEG was found to have crystalline nature with two clear diffraction peaks (Fig. 4b). Instead, PVP was found to be amorphous showing a halo diffraction pattern (Fig. 4c). All the characteristic peaks of PPZ were found to be absent in the diffraction spectrum of freeze-dried PPZ, indicating amorphization of PPZ as a consequence of the freeze-drying process (Fig. 4d). No characteristic diffraction peaks of PPZ were observed in the diffraction patterns of the prepared PPZ/PVP solid dispersions which was evidence for the presence of PPZ in an amorphous form in these dispersions (Fig. 5a–c). An amorphous hump was clearly caused by PVP since its intensity increased as the amount of PVP in the dispersions increased. Instead, in all of the diffraction patterns of the prepared PPZ/PEG dispersions (Fig. 5d–f), two distinctive diffraction peaks (approx. at 2θ of 19.2 and 23.3) were observed. Since the diffraction peaks of the PPZ/PEG solid dispersions appeared at similar 2θ values as the peaks of the pure PEG, their intensity increased as the amount of PEG in the dispersions increased and no diffractions at the characteristic 2θ values of PPZ were observed, the peaks were attributable only to the presence of crystalline PEG in the solid dispersions.

In the DSC measurements (Table 3), pure PPZ showed the melting endotherm at 97.8 °C and the glass transition (T_g) at 15.3 °C (second heating phase). Amorphous PVP showed a T_g at 172 °C (second heating phase). Instead, the thermogram of PEG displayed only melting (T_m) at 59.6 °C. However, a T_g-value of −55 °C has been observed for PEG 8000 [8]. Thus, PEG used in this study is either fully crystalline or T_g of the possible amorphous portion was out of the measurement range of the DSC instrument. A striking difference was observed between the T_g-value of pure PPZ (obtained from the second heating phase of DSC-measurement for pure PPZ, see Table 1) and the *T_g-value* for freeze-dried, amorphous PPZ (Table 3). This is attributable to the formation of amorphous PPZ hydrochloride salt during the freeze-drying process (formation of PPZ dihydrochloride was confirmed by elemental analysis). The obtained DSC thermograms of physical mixtures and corresponding solid dispersions (not shown) differed significantly from each other indicating that changes had occurred in the physical state of the materials (Table 3). Melting endotherms of PPZ and T_g-values of PVP, corresponding to the T_g of pure PVP, were clearly visible in all PPZ/PVP physical mixtures. In the thermograms of the corresponding solid dispersions, the T_m of PPZ had disappeared and no T_m of PPZ hydrochloride salt was seen either, due to amorphization of PPZ, observed by XRPD. A single T_g between the T_g-values of the components was observed, confirming the formation of a solid

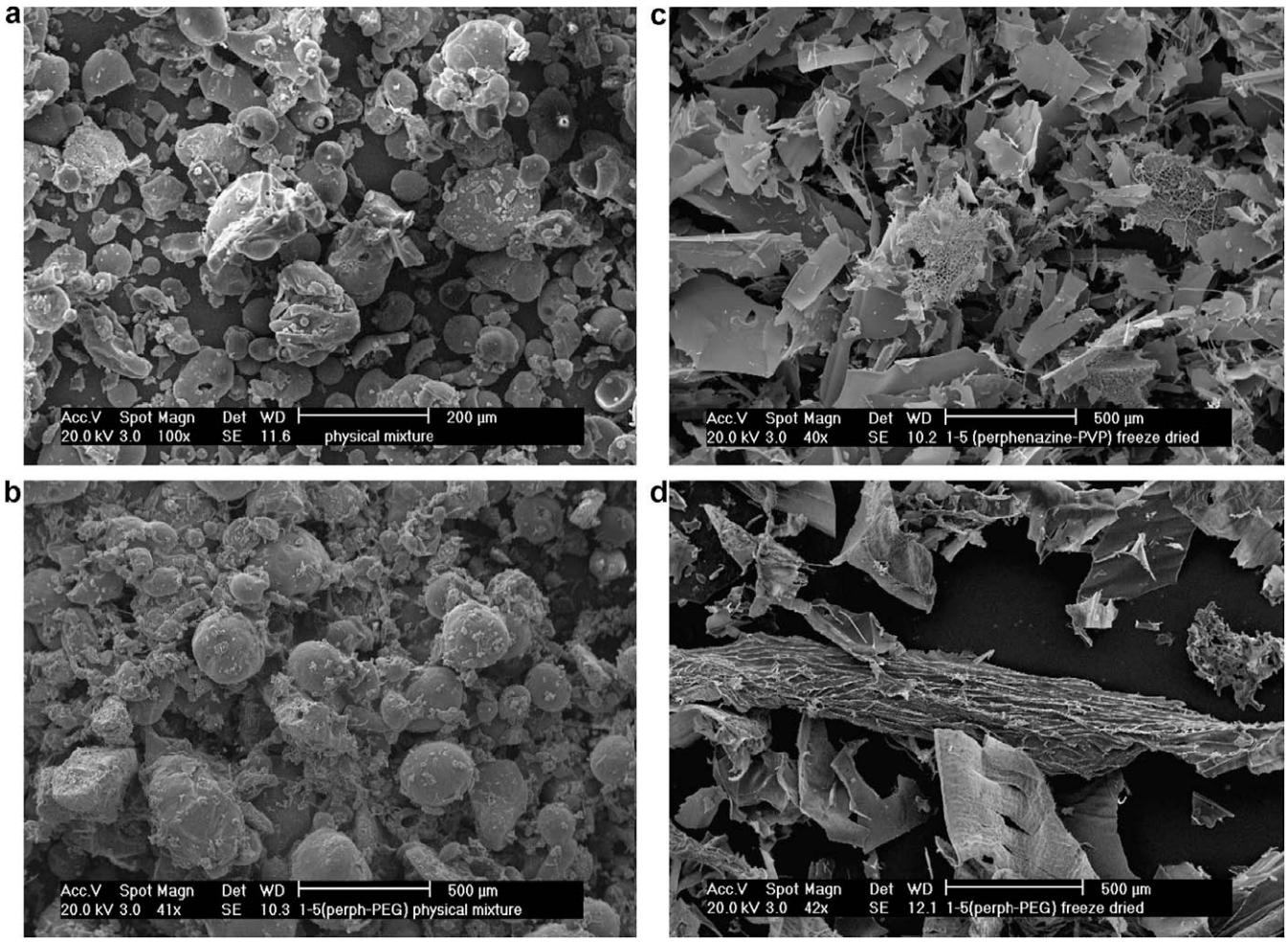

Fig. 3. Scanning electron micrographs of physical mixture of (a) PPZ and PVP (1/5 m/m); (b) PPZ and PEG (1/5 m/m); and solid dispersion of (c) PPZ and PVP (1/5 m/m); (d) PPZ and PEG (1/5 m/m).

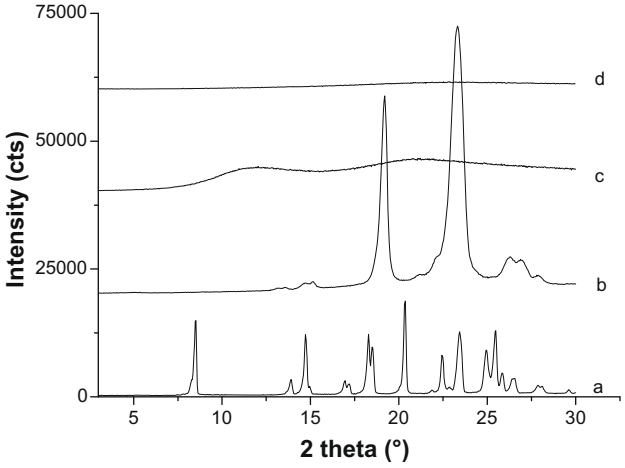

Fig. 4. X-ray diffraction patterns of (a) PPZ; (b) PEG; (c) PVP; (d) freeze-dried PPZ.

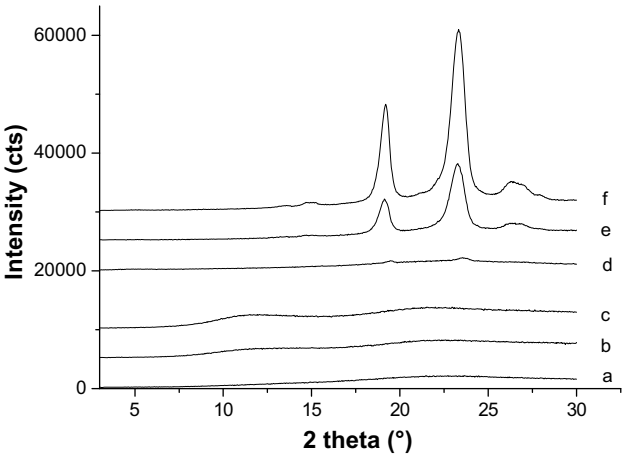

Fig. 5. X-ray diffraction patterns of (a) 5/1 PPZ/PVP; (b) 1/5 PPZ/PVP; (c) 1/20 PPZ/PVP; (d) 5/1 PPZ/PEG; (e) 1/5 PPZ/PEG; (f) 1/20 PPZ/PEG.

solution [8]. Instead, in the case of PPZ/PEG, the T_m of PPZ was clearly seen in the thermogram of 5/1 physical mixture. In the 1/5 mixture it was barely distinguishable from the baseline and in the 1/20 mixture, it had disappeared completely. This phenomenon is indicative of PPZ dissolving into the melted PEG during heating [28]. In the thermograms of the PPZ/PEG dispersions, no T_m of PPZ was seen, which based on XRPD, was known to be due to amorphization of PPZ instead of PPZ dissolving into the melted PEG. In addition, a single T_g (Table 3) could be detected for all PPZ/PEG dispersions, but also the T_m of PEG was visible (Table 4). Interestingly, compared to the corresponding physical mixtures, the ΔH values of the PEG melting endotherms were lower in the

Table 3
Melting points (T_m) and glass transition temperatures (T_g) of pure PPZ, PVP and PEG, freeze-dried PPZ, 5/1, 1/5 and 1/20 PPZ/PVP and PPZ/PEG solid dispersions, and the corresponding physical mixtures

Sample	T_m (°C)	T_m of PPZ in physical mixture (°C)	T_m of polymer in physical mixture (°C)	T_g (°C)	T_g of the solid dispersion (°C)
PPZ	97.8 ± 0.3	–	–	15.3 ± 0.3	–
PVP	nd	–	–	172 ± 0.3	–
PEG	59.6 ± 0.2[a]	–	–	nd	–
Freeze-dried PPZ	nd	–	–	–	53.8 ± 2.5
5/1 PPZ/PVP	–	97.3 ± 0.2	–	–[b]	58.9 ± 0.6
1/5 PPZ/PVP	–	95.5 ± 1.3	–	173.4 ± 0.8[b]	155.1 ± 2.4
1/20 PPZ/PVP	–	96.9 ± 0.5	–	172.0 ± 0.7[b]	170.3 ± 1.3
5/1 PPZ/PEG	–	94.8 ± 0.5	59.7 ± 0.1	nd[b]	22.2 ± 0.7
1/5 PPZ/PEG	–	95.8 ± 0.2	59.3 ± 0.1	nd[b]	−44.9 ± 0.2
1/20 PPZ/PEG	–	nd	59.4 ± 0.1	nd[b]	nd

nd, not detected.
–, not determined.
[a] ΔH = 186 ± 3 J/g.
[b] Physical mixture.

Table 4
Melting points (T_m) and melting enthalpies (ΔH) of PEG in the PPZ/PEG physical mixtures and prepared solid dispersions

Sample	T_m of PEG in physical mixture (°C)	ΔH of PEG in physical mixture (J/g)[a]	T_m of PEG in solid dispersion (°C)	ΔH of PEG in solid dispersion (J/g)[a]
5/1 PPZ/PEG	59.7 ± 0.1	165 ± 20	62.9 ± 0.1	9.4 ± 2.0
1/5 PPZ/PEG	59.3 ± 0.1	198 ± 7	61.4 ± 1.2	157 ± 6
1/20 PPZ/PEG	59.4 ± 0.1	193 ± 1	61.2 ± 0.3	168 ± 2

[a] ΔH is corrected for the amount of PEG in the mixture.

solid dispersions (i.e. the increase in the proportional amount of amorphus PEG) and decreased linearly as a function of PPZ content (Table 4), indicating lattice distortion of the carrier due to the formation of a solid solution [15]. Furthermore, the melting temperature of PEG was higher in the dispersions (Table 4) which might be attributable to that the higher melting (extended chain) form of PEG remained crystalline while the lower melting, once folded modification transformed to the amorphous form [34]. The amount of amorphized PEG was found to be 94%, 21% and 13% for 5/1, 1/5 and 1/20 dispersions, respectively, as can be calculated from the ΔH values in Table 4 and the ΔH value for pure PEG (Table 3). Thus, the formulations consisted of two phases; one composed of crystalline PEG and one of amorphous PPZ/PEG containing 19%, 38% and 65% of amorphous PEG, respectively.

The theoretical T_g-value for each of the drug–polymer blends can be calculated according to the Gordon–Taylor equation [26,35,36]:

$$T_{g12} = \frac{w_1 T_{g1} + K w_2 T_{g2}}{w_1 + K w_2} \quad (1)$$

where T_{g12} is the glass transition temperature of the drug–polymer blend, w_1, w_2, T_{g1} and T_{g2} are the weight fractions and glass transition temperatures (K) of the pure drug and polymer, respectively. K is a constant describing the interaction between the components and it can be approximated using the following equation (Simha-Boyer rule):

$$K \approx \frac{\rho_1 T_{g1}}{\rho_2 T_{g2}} \quad (2)$$

where ρ_1 and ρ_2 are the true densities of the components. The T_gs of the freeze-dried PPZ and PVP measured by DSC (Table 3) and the T_g-value from literature for PEG [8] were used for the calculations. The true density of the components was measured by helium pycnometry, obtained values being 1.31, 1.17 and 1.48 g/cm^3 for PPZ; PVP and PEG, respectively. Furthermore, in the calculations for PPZ/PEG mixtures, the true compositions of amorphous PPZ/PEG phase were used. The T_g-values observed by DSC were found to be in reasonable agreement with the values predicted for the solid dispersions by the Eq. (1) (Fig. 6), except the value for 1/5 PPZ/PEG. Generally, deviation from ideal behavior would be caused by differences in strength of intermolecular interactions between the individual components and those of the blend [26].

3.2.3. Evaluation of the drug–polymer interactions

The observed molecular dispersion of PPZ into the PVP or PEG matrix might be promoted by interactions between PPZ and the polymers. These interactions give rise to band shifts and broadening of the peaks characteristic for the interacting groups compared to the FTIR spectra of the corresponding physical mixtures.

The spectra of the pure compounds show absorptions of the potential hydrogen bonding groups (Fig. 7a). The OH-group of PPZ is a hydrogen bond donor and might thus be able to be involved in intermolecular interactions [OH-bands at 3488 and 1054 cm^{-1} (C–O stretch)]. In the case of PVP, the carbonyl group (band at 1655 cm^{-1}) is the hydrogen bonding group, since the interaction of the >N-group (C–N band for tertiary amines at 1284 cm^{-1}) is sterically hindered [16]. A very broad band observed around 3400 cm^{-1}, indicating the presence of water, revealed the hygroscopic nature of PVP [37]. The potential hydrogen bonding sites of PEG are the lone pairs of the oxygen atoms (C–O stretching (ether) at 1094 cm^{-1}).

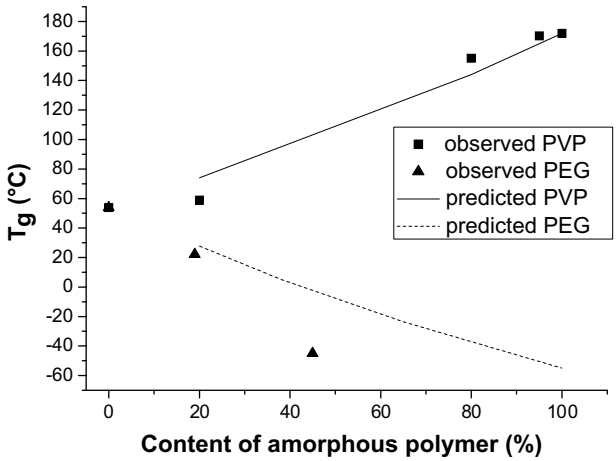

Fig. 6. T_g-values of freeze-dried perphenazine, 5/1, 1/5 and 1/20 PPZ/PVP and PPZ/PEG solid dispersions observed by DSC measurements [PVP (■) and PEG (▲)] and predicted by Gordon-Taylor equation [PVP (—) and PEG (– – –)]. In the case of PPZ/PEG dispersions, the true compositions of the amorphous PPZ/PEG phases are used.

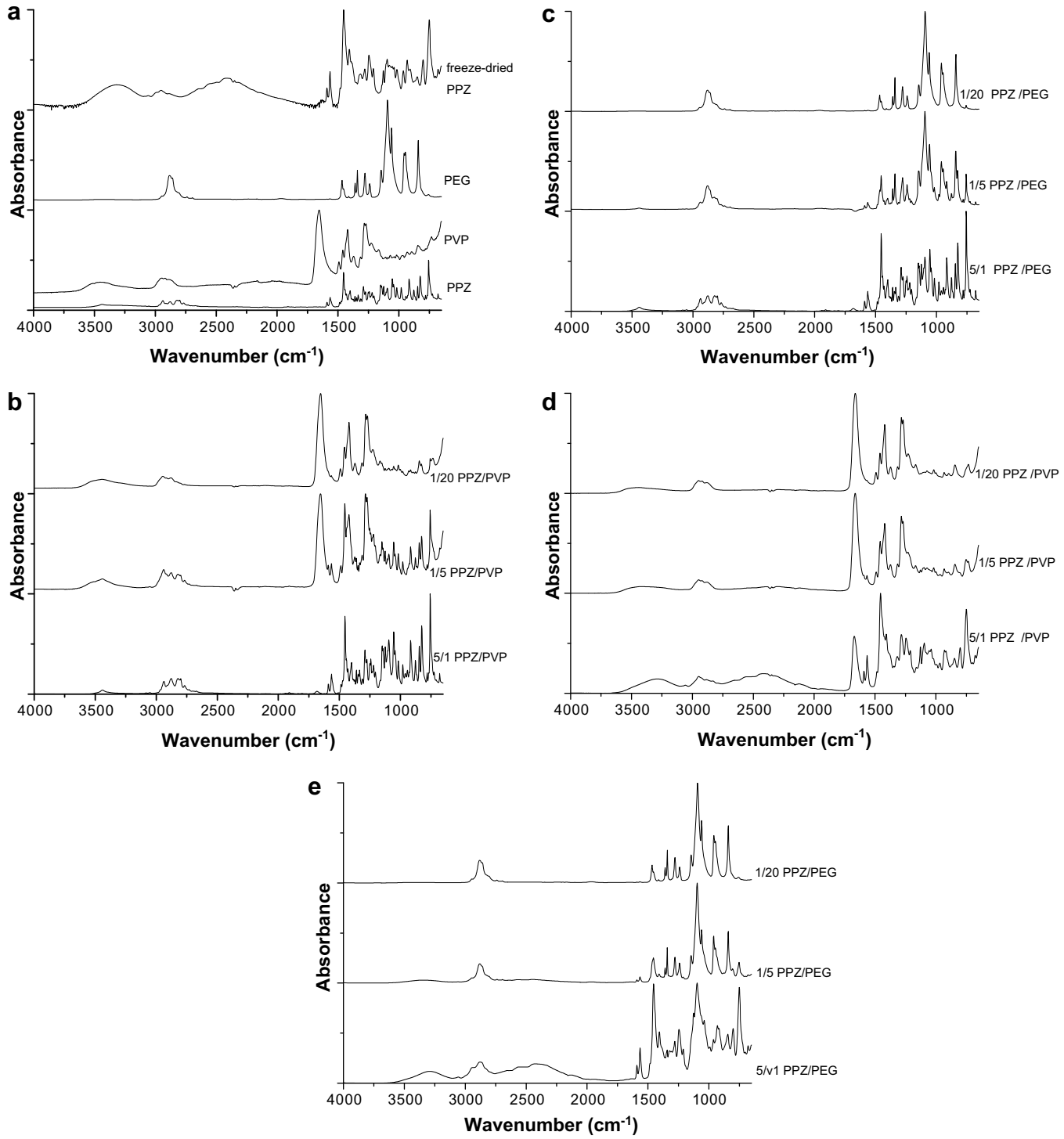

Fig. 7. The FTIR spectra of (a) pure PPZ, PVP, PEG and freeze-dried PPZ; (b) the physical mixtures: 5/1 PPZ/PVP, 1/5 PPZ/PVP, 1/20 PPZ/PVP; (c) the physical mixtures: 5/1 PPZ/PEG, 1/5 PPZ/PEG and 1/20 PPZ/PEG; (d) the solid dispersions: 5/1 PPZ/PVP, 1/5 PPZ/PVP, 1/20 PPZ/PVP; (e) the solid dispersions: 5/1 PPZ/PEG, 1/5 PPZ/PEG and 1/20 PPZ/PEG.

In the case of freeze-dried PPZ (Fig. 7a), OH-band (at 3488 cm^{-1} in the spectrum of pure PPZ, Fig. 7a) had broadened, which is an evidence of an interaction with water due to the increased water content of the material. Also, a new broad absorption was observed around 2400 cm^{-1} (H–Cl stretching absorption) which is probably indicative of the formation of HCl salt of PPZ due to the preparation method. In general, the absorption peaks appeared to be less sharp in the spectrum of freeze-dried PPZ, pointing to the formation of amorphous material.

The spectra of the PPZ/polymer physical mixtures (Fig. 7b and c) seemed to correspond to the sum spectra of the pure compounds. Instead, in the spectra of the solid dispersions (Fig. 7d and e) changes compared to the physical mixtures were observed. In the case of the PPZ/PVP dispersions, general broadening of the peaks was observed compared to the physical mixtures (Fig. 7b and d). The OH-bands of PPZ at 3488 cm^{-1} were replaced by broader and less intense bands and the C–O stretching absorptions of PPZ at 1054 cm^{-1} had disappeared in all of the solid dispersions.

The intense carbonyl band of PVP at 1655 cm^{-1} in the physical mixtures, had shifted to 1670, 1663 and 1662 cm^{-1} in the 5/1, 1/5 and 1/20 dispersions, respectively. This was a clear indication of involvement of OH-groups of PPZ and carbonyl groups of PVP in the intermolecular hydrogen bonding, which might stabilize the amorphous structure of the PPZ/PVP dispersions [38]. However, usually the carbonyl shift occurs to lower wave numbers [26], but similar shifts to higher wave numbers, indicating specific drug–PVP interactions, have been also observed [16,39]. In addition, a new absorption peak around 2400 cm^{-1}, as in the case of freeze-dried PPZ, was observed with PPZ/PVP dispersions. This was attributed to presence of HCl (due to the preparation method) and it became less distinctive from the baseline as the intensity of the PVP absorptions increased with the higher amounts of PVP present in the dispersion.

In the case of PPZ/PEG solid dispersions, the changes in spectra compared to the physical mixtures were not so distinctive (Fig. 7c and e) (Fig. 6). An indication of hydrogen bond formation in the case of 5/1 and 1/5 dispersions was the broadening of the OH-band of PPZ (at 3488 cm^{-1}). However, in the case of 1/20 PPZ/PEG, this band could not be distinguished from the baseline even in the spectrum of the physical mixture. Also, a small shift of the C–O stretching band (~2 cm^{-1} to the higher wavenumbers) was observed in the case of 5/1 and 1/5 formulations. In addition, also here the absorption around 2400 cm^{-1} (attributed to the presence of HCl) appeared in the spectrum of the dispersions, becoming less distinctive when more PEG was present in the dispersion due to increase in the intensity of the PEG absorptions.

4. Discussion

PPZ is a first-generation antipsychotic with low aqueous solubility (i.e. lower than 150 μg/ml at pH 6.8) and poor dissolution rate (Fig. 1a). Formulation of PPZ into an intraoral formulation would be useful e.g. in order to achieve a rapid onset of action, however, this would require enhanced solubility and dissolution rate of PPZ in the conditions present in the oral cavity (i.e. low amount of saliva and pH 6.2–7.4). In this study, a solid dispersion approach was found to be an effective means for increasing the dissolution rate of PPZ. By choosing polymer carriers so that they have the solubility parameters similar to that of PPZ (i.e. PVP K30 and PEG 8000) suitable conditions were achieved for molecular mixing of PPZ with the carriers. The improvement of the dissolution rate can be illustrated by the time required for dissolving 50% of PPZ (T_{50}). 1/5 and 1/20 PPZ/PEG dispersions and freeze-dried PPZ had superior dissolution (T_{50} < 15 s, Fig. 1d) compared to the other solid dispersions (T_{50} > 50 s). With respect to the PVP dispersions, the 1/5 formulation seemed to have the best T_{50} value (50 s, Fig. 1c).

Usually, the dissolution rate of solid dispersions increases with increasing polymer content due to the solubilizing effect of the polymer and amorphization of the drug only at low drug loads [37–43]. Since in this study, PPZ was found to be amorphous at all mixture ratios, as confirmed by XRPD (Figs. 4 and 5) and DSC (Table 3), this phenomenon was not seen here. In addition, in studies with other drugs, it has been observed that often the dissolution rate of a drug is similar from PEG and PVP solid dispersions, probably due to their similar dissolution enhancing mechanisms [37,44]. The different behavior observed in this study was probably attributable to the poorer wettability of the PPZ/PVP powders, this being observed visually since the PPZ/PVP powders remained floating on the liquid surface. This result was surprising, since generally improved wettability by PVP has been considered as one of the main factors which hastens the dissolution of drugs [7,45]. The observed poor wettability might be due to the preparation process (freeze-drying), which might electrically charge the powder. Also, PVP is known to be hygroscopic [37] and thus a high hygroscopicity of the particles, causing absorption of ambient moisture and aggregation of the particles, might lead to a reduced surface area and poor wettability [46], which might explain the poor dissolution rate of PPZ also from 5/1 PPZ/PVP and PPZ/PEG dispersions. These two formulations seemed to absorb ambient moisture, which led to stickiness and reduced wettability of the powders making them very difficult to handle under laboratory conditions. PVP has also been observed to act as a binder with some drugs which could cause decreased dissolution rate [47]. Furthermore, at high polymer contents, PVP might form a viscous layer during dissolution, hindering the dissolution of the drug [33]. These facts might explain the slower dissolution of PPZ from 1/20 PPZ/PVP compared to 1/5 PPZ/PVP.

When studying the distribution of PPZ in 1/5 and 1/20 PPZ/polymer dispersions with SAXS, it was found that PPZ, incorporated into the polymer, was "invisible" to the equipment and it can be assumed that instead of being present as clusters in the dispersion, PPZ was dispersed as individual molecules in both polymers, evidence for the formation of a homogenous solid solution (Fig. 2a and b). Furthermore, no difference between 1/5 and 1/20 dispersions was observed contrary to some previous studies with SEM, TEM or micro-Raman, where drug particle size decreased as the amount of polymer in the dispersion increased [9,12]. The assumption of solid solution formation was confirmed by XRPD and DSC studies (Figs. 4 and 5, Table 3), which revealed that PPZ was present in an amorphous form in the dispersions in all mixture ratios and that all the dispersions had a single T_g, in contrast to many studies with other drugs where amorphization of the drug has occurred only at higher polymer contents [40–42]. This was probably due to the complete miscibility of PPZ with the carriers, due to the similarity of their solubility parameters. A decrease in PEG crystallinity as a function of increasing PPZ content was also seen in DSC (Table 4). A decrease in PEG crystallinity as a consequence of solid dispersion formation has been previously reported [19,43,48] with other drugs. From these results it could be concluded that PPZ formed amorphous molecular dispersions with fully amorphous PVP or with the amorphous part of PEG, which was calculated to be 95, 16 and 10% for 5/1, 1/5 and 1/20 PPZ/PEG mixtures, respectively (Table 4).

The unexpectedly high T_g-value observed for the amorphous, freeze-dried PPZ (Table 3) was attributed to the formation of amorphous PPZ dihydrochloride salt due to the preparation method, where PPZ was dissolved in 0.1 N HCl solution for the solubility reasons. Salt formation and the subsequent ionic interaction between drug and different counterions have been previously observed to result in very high T_g-values [49,50]. FTIR results revealed that hydrogen bonding between PPZ and PVP and/or HCl promoted the formation of PPZ/PVP solid solutions. In accordance with the previous studies done on other drugs, it was difficult to demonstrate hydrogen bonding between PPZ and PEG from the FTIR spectra of the dispersions [17,37], though it was considered likely. However, the FTIR results confirmed the presence of HCl salt in the dispersions.

Thus according to the above results, formation of a solid solution of PPZ may not be the only factor enhancing the drug dissolution from the solid dispersions. In addition, the presence of PPZ HCl salt in the solid dispersions created a microenvironment around the dissolving particles which led to a high supersaturation of PPZ. This promoted the dissolution of PPZ, especially in the case of high drug-loaded dispersions (5/1 PPZ/polymer). Also earlier, simultaneous modulation of the microenvironmental pH and drug crystallinity in solid dispersions has been found to be a useful way to increase the dissolution rate of an ionizable drug [51,52].

5. Conclusions

In this study, freeze-drying of solutions of a poorly water soluble PPZ with 0%, 20%, 80% or 95% of a polymer led to an improved PPZ solubility and extremely fast dissolution rate in a small liquid (pH 6.8) volume compared to crystalline or micronized PPZ. The most remarkable improvement in the dissolution rate was seen with 1/5 PPZ/PEG dispersion, which dissolved within one minute without precipitation of the supersaturated PPZ. SAXS measurements suggested that PPZ was molecularly dispersed within the 1/5 and 1/20 PPZ/polymer matrices, since the addition of PPZ into the polymer matrix did not change the size distribution of the inhomogeneity regions to any significant extent compared to the polymers alone. Single T_g-values observed with DSC for every mixture ratio and XRPD measurements further supported molecular mixing and confirmed the presence of amorphous PPZ in of the dispersions. Solid solution formation was promoted by hydrogen bonding interactions between the drug and polymers, the existence of which was confirmed by FTIR. Interestingly, in the case of freeze-dried PPZ, a considerable increase in T_g was observed, due to the formation of amorphous PPZ hydrochloride salt which was also detected by FTIR. It can be concluded that the formation of HCl salt and solid solutions promoted the dissolution of PPZ, especially in the case of the 1/5 PPZ/PEG dispersion, which makes it a promising candidate for further studies, including stability studies, on the way to achieving intraoral formulations.

Acknowledgements

The financial support by Finnish Funding Agency of Technology and Innovation (Tekes) and Kuopio University Pharmacy is gratefully acknowledged. R.L. thanks the Finnish Cultural Foundation for financial support. The expert technical advice of Ph.D. Ossi Korhonen during the DSC studies is gratefully acknowledged.

Appendix A. Supplementary data

Supplementary data associated with this article can be found, in the online version, at doi:10.1016/j.ejpb.2008.09.001.

References

[1] I.W. Kellaway, G. Ponchel, D. Duchene, Oral mucosal drug delivery, in: M. Rathbone (Ed.), Modified-release Drug Delivery Technology, Marcel Dekker, Inc, New York, USA, 2002, pp. 349–364.
[2] L. Dobetti, Fast-melting tablets: developments and technologies, Phar. Tech. Feb. 2 (2001) 44–50.
[3] S. Bredenberg, M. Duberg, B. Lennernäs, H. Lennernäs, A. Pettersson, M. Westerberg, C. Nyström, In vitro and in vivo evaluation of a new sublingual tablet system for rapid oromucosal absorption using fentanyl citrate as the active substance, Eur. J. Pharm. Sci. 20 (2003) 327–334.
[4] A.C. Jain, B.J. Aungst, M.C. Adeyeye, Development and in vivo evaluation of buccal tablets prepared using danazol-sulfobutylether 7 β-cyclodextrin (SBE 7) complexes, J. Pharm. Sci. 91 (2002) 1659–1668.
[5] C. Leuner, J. Dressman, Improving drug solubility for oral delivery using solid dispersions, Eur. J. Pharm. Biopharm. 50 (2000) 47–60.
[6] S. Sethia, E. Squillante, Solid dispersions: revival with greater possibilities and applications in oral drug delivery, Crit. Rev. Therap. Drug. Carrier Syst. 20 (2003) 215–247.
[7] W.L. Chiou, S. Riegelman, Pharmaceutical applications of solid dispersion systems, J. Pharm. Sci. 60 (1971) 1281–1302.
[8] A. Forster, J. Hempenstall, I. Tucker, T. Rades, Selection of excipients for melt extrusion with two poorly water-soluble drugs by solubility parameter calculation and thermal analysis, Int. J. Pharm. 226 (2001) 147–161.
[9] E. Karavas, G. Ktistis, A. Xenakis, E. Georgarakis, Effect of hydrogen bonding interactions on the release of felodipine from nanodispersions with polyvinylpyrrolidone, Eur. J. Pharm. Sci. 63 (2006) 103–114.
[10] S.K. Dordunoo, J.L. Ford, M.H. Rubinstein, Physical stability of solid dispersions containing triamterene or temazepam in polyethylene glycols, J. Pharm. Pharmacol. 49 (1997) 390–396.
[11] S. Verheyen, N. Blaton, R. Kinget, G. Van den Mooter, Mechanism of increased dissolution of diazepam and temazepam from polyethylene glycol 600 solid dispersions, Int. J. Pharm. 249 (2002) 45–58.
[12] E. Karavas, M. Georgarakis, A. Docoslis, D. Bikiaris, Combining SEM, TEM and micro-Raman techniques to differentiate between the amorphous molecular level dispersions and nanodispersions of a poorly water-soluble drug within a polymer matrix, Int. J. Pharm. 340 (2007) 76–83.
[13] C. Guozhong (Ed.), Characterization and properties of nanomaterials, Nanostructures and Nanomaterials, World Scientific Publishing Company Inc., Singapore, 2004, pp. 333–336.
[14] H. Konno, L.S. Taylor, Influence of different polymers on the crystallization tendency of molecularly dispersed amorphous felodipine, J. Pharm. Sci. 95 (2006) 2692–2705.
[15] D. Law, S.L. Krill, E.A. Schmitt, J.J. Fort, Y. Qiu, W. Wang, W.R. Porter, Physicochemical considerations in the preparation of amorphous ritonavir-poly(ethylene glycol) 8000 Solid dispersions, J. Pharm. Sci. 90 (2001) 1015–1025.
[16] L.S. Taylor, G. Zografi, Spectroscopic characterization of interactions between PVP and indomethacin in amorphous molecular dispersions, Pharm. Res. 14 (1997) 1691–1698.
[17] S. Anguiano-Igea, F.J. Otero-Espinar, J.L. Vila-Jato, J. Blanco-Mendez, The properties of solid dispersions of clofibate in polyethylene glycols, Pharm. Acta Helv. 70 (1995) 57–66.
[18] N.A. Urbanetz, B.C. Lippold, Solid dispersions of nimodipine, polyethylene glycol 2000 Dissolution properties and physico-chemical characterization, Eur. J. Pharm. Biopharm. 59 (2005) 107–118.
[19] I. Weuts, D. Kempen, G. Verreck, A. Decorte, K. Heymans, J. Peeters, M. Brewster, G. Van den Mooter, Study of the physicochemical properties, stability of solid dispersions of loperamide, PEG 6000 Prepared by spray drying, Eur. J. Pharm. Biopharm. 59 (2005) 119–126.
[20] A.C. Moffat, M.D. Osselton, B. Widdop (Eds.), Clarke's Analysis of Drugs and Poisons, Pharmaceutical Press, London, Great Britain, 2006.
[21] D.J. David, A. Misra (Eds.), Cohesive properties and solubility parameter concepts, Relating Materials Properties to Structure. Handbook and Software for Polymer Calculations and Materials Properties, Lancaster Technomic Publishing Co. Inc., USA, 1999, pp. 287–304.
[22] D.J. Greenhalg, A.C. Williams, P. Timmins, P. York, Solubility parameters as predictors of miscibility in solid dispersions, J. Pharm. Sci. 88 (1999) 1182–1190.
[23] P.J. Marsac, S.L. Shamblin, L.S. Taylor, Theoretical and practical approaches for prediction of drug–polymer miscibility and solubility, Pharm. Res. 23 (2006) 2417–2426.
[24] B. Hancock, P. York, R. Rowe, The use of solubility parameters in pharmaceutical dosage form design, Int. J. Pharm. 148 (1997) 1–21.
[25] D.W. Van Krevelen (Ed.), Cohesive properties and solubility, Properties of Polymers. Their Correlation with Chemical Structure: Their Numerical Estimation and Prediction from Additive Group Contributions, Elsevier, Amsterdam, The Netherlands, 1997, pp. 189–225.
[26] R. Nair, N. Nyamweya, S. Gönen, L.J. Martinez-Miranda, S.W. Hoag, Influence of various drugs on the glass transition temperature of poly(vinylpyrrolidone): a thermodynamic and spectroscopic investigation 225 (2001) 83–96.
[27] M. Langer, M. Höltje, N.A. Urbanetz, B. Brandt, H.D. Höltje, B.C. Lippold, Investigations on the predictability of the formation of glassy solid solutions of drugs in sugar alcohols, Int. J. Pharm. 252 (2003) 167–179.
[28] P. Mura, J.R. Moyano, M.L. Gonzales-Rodriquez, A.M. Rabasco-Alvarez, M. Cirri, F. Maestrelli, Characterization and dissolution properties of ketoprofen in binary and ternary solid dispersions with polyethylene glycol and surfactants, Drug. Dev. Ind. Pharm. 31 (2005) 425–434.
[29] S. Sethia, E. Squillante, Solid dispersion of carbamazepine in PVP K30 by conventional solvent evaporation and supercritical methods, Int. J. Pharm. 272 (2004) 1–10.
[30] L.P. Ruan, B.Y. Yu, G.M. Fu, D. Zhu, Improving the solubility of ampelopsin by solid dispersions and inclusion complexes, J. Pharm. Biomed. Anal. 38 (2005) 457–464.
[31] C.B. Murray, C.R. Kagan, M.G. Bawendi, Synthesis and characterization of monodisperse nanocrystals and close-packed nanocrystal assemblies, Annu. Rev. Mater. Sci. 30 (2000) 545–610.
[32] K.S. Finnie, J.R. Bartlett, C.J. Barbe, L. Kong, Formation of silica nanoparticles in microemulsions, Langmuir 23 (2007) 3017–3024.
[33] D.Q.M. Craig, The mechanisms of drug release from solid dispersions in water-soluble polymers, Int. J. Pharm. 231 (2002) 131–144.
[34] D.Q.M. Craig, Polyethylene glycols and drug release, Drug. Dev. Ind. Pharm. 16 (1990) 2501–2526.
[35] M. Gordon, J.S. Taylor, Ideal copolymers and the second order transition of synthetic rubbers 1. Non-crystalline co-polymers, J. Appl. Chem. 2 (1952) 493–500.
[36] Q. Lu, G. Zografi, Phase behavior of binary and ternary amorphous mixtures containing indomethacin, citric acid and PVP, Pharm. Res. 15 (1998) 1202–1206.
[37] G. Van den Mooter, P. Augustinjs, N. Blaton, R. Kinget, Physico-chemical characterization of solid dispersions of temazepam with polyethylene glycol 6000 and PVP K30, Int. J. Pharm. 164 (1998) 67–80.
[38] T. Matsumoto, G. Zografi, Physical properties of solid molecular dispersions of indomethacin with poly(vinylpyrrolidone) and poly(vinylpyrrolidone-co-vinylacetate) in relation to indomethacin crystallization, Pharm. Res. 14 (1999) 1722–1728.
[39] E. Karavas, G. Ktistis, A. Xenakis, E. Georgarakis, Miscibility behavior and formation mechanism of stabilized felodipine-polyvinylpyrrolidone amorphous solid dispersions, Drug. Dev. Ind. Pharm. 31 (2005) 473–489.

[40] A. Paradkar, A.A. Ambike, B. Jadhav, K.R. Mahadik, Characterization of curcumin-PVP solid dispersion obtained by spray drying, Int. J. Pharm. 271 (2004) 281–286.
[41] J. Shah, J. Chen, D. Chow, Preformulation study of etoposide. II: increased solubility and dissolution rate by solid–solid dispersion, Int. J. Pharm. 113 (1995) 103–111.
[42] C.W. Lin, T.M. Cham, Effect of particle size on the available surface area of nifedipine from nifedipine-polyethylene glycol 600 solid dispersions, Int. J. Pharm. 127 (1996) 261–272.
[43] S.G. Vijaya Kumar, D.N. Mishra, Preparation, characterization and in vitro dissolution studies of solid dispersion of meloxicam with PEG 6000, Yakugaku Zasshi 126 (2006) 657–664.
[44] C.Y. Perng, A.S. Kearney, K. Patel, N.R. Palepu, G. Zuber, Investigation of formulation approaches to improve the dissolution of SB-210661, a poorly water soluble 5-lipoxygenase inhibitor, Int. J. Pharm. 176 (1998) 31–38.
[45] R.P. Patel, M.M. Patel, Physicochemical characterization, dissolution study of solid dispersions of lovastatin with polyethylene glycol 4000 and polyvinylpyrrolidone K30, Pharm, Dev. Technol. 12 (2007) 21–33.
[46] N. Elkhider, K.L.A. Chan, S.G. Kazarian, Effect of moisture and pressure on tablet compaction studied with FTIR spectroscopic imaging, J. Pharm. Sci. 96 (2007) 351–360.
[47] S.S. Bansal, A.M. Kaushal, A.K. Bansal, Molecular and thermodynamic aspects of solubility advantage from solid dispersions, Mol. Pharm. 4 (2007) 794–802.
[48] P. Mura, M.T. Faucci, A. Manderioli, G. Bramanti, P. Parrini, Thermal behavior and dissolution properties of naproxen from binary and ternary solid dispersions, Drug Dev. Ind. Pharm. 25 (1999) 257–264.
[49] P. Tong, G. Zografi, Solid-state characterization of amorphous sodium indomethacin relative to its free acid, Pharm. Res. 16 (1999) 1186–1192.
[50] P. Tong, L.S. Taylor, G. Zografi, Influence of alkali metal counterions on the glass transition temperature of amorphous indomethacin salts, Pharm. Res. 19 (2002) 649–654.
[51] F. Usui, K. Maeda, A. Kusai, M. Ikeda, K. Nishimura, K. Yamamoto, Dissolution improvement of RS-8350 by the solid dispersion prepared by the solvent method, Int. J. Pharm. 170 (1998) 247–256.
[52] P.H. Tran, H.T. Tran, B.J. Lee, Modulation of microenvironmental pH and crystallinity of ionizable telmisartan using alkalizers in solid dispersions for controlled release, J. Control. Rel. 129 (2008) 59–65.